

M F F Nave et al

# Plasma Current Dependence of the Edge Pedestal Height in JET ELM-free H-modes



# Plasma Current Dependence of the Edge Pedestal Height in JET ELM-free H-modes

M F F Nave<sup>1</sup>, P Lomas, C Gowers, H Guo,  
N Hawkes, G T A Huysmans<sup>2</sup>, T Jones, V V Parail,  
F Rimini, B Schunke<sup>2</sup>, P Thomas.

JET Joint Undertaking, Abingdon, Oxfordshire, OX14 3EA,

<sup>1</sup>Associação EURATOM/IST, Lisboa, Portugal.

<sup>2</sup>present address: CEA/Cadarache, St. Paul-lez-Durance, France.

Preprint of a Paper to be submitted for publication in  
Plasma Physics and Controlled Fusion

January 2000

"This document is intended for publication in the open literature. It is made available on the understanding that it may not be further circulated and extracts may not be published prior to publication of the original, without the consent of the Publications Officer, JET Joint Undertaking, Abingdon, Oxon, OX14 3EA, UK".

"Enquiries about Copyright and reproduction should be addressed to the Publications Officer, JET Joint Undertaking, Abingdon, Oxon, OX14 3EA".

## ABSTRACT

Models for the suppression of turbulence in the L to H transition, suggest that the width of the H-mode edge barrier is either proportional or is of the order of the ion poloidal Larmor radius. This would require that the width of the edge barrier should depend on the plasma current. This dependence has been clearly verified at JET in experiments designed to control the edge MHD stability of ELM-free hot-ion H-mode plasmas. The effects of isotopic mass and the applicability of several edge barrier models to the hot-ion H-mode plasmas were analysed in [1] using a large database containing both Deuterium-only (DD) and Deuterium-Tritium (DT) plasmas. This database has now been enlarged to include discharges from a plasma shape scan, allowing to study the dependence of the pedestal height on the edge shear. In addition the range of plasma currents was extended up to 6 MA. It is shown that the edge data is best described by a model where the edge barrier width is determined by the fast ions weighted towards the components with largest poloidal Larmor radii. However, it is not possible to eliminate conclusively the thermal ion model.

## INTRODUCTION

Hot-ion H-mode plasmas are characterised by an ELM-free period, lasting up to a few seconds, when the total plasma stored energy, as well as the edge pedestal pressure, rise until limited by a MHD event. The plasma current,  $I_p$ , was found to be a key parameter on the control of both Outer Modes (OMs) and the onset of the first giant ELM. The effect of changing the plasma current on the edge and global pressures, as well as on the duration of the ELM-free period has been studied in two types of experiments [2]: current ramp-down experiments to suppress the OM and plasma current scans to control the ELM-free period. Edge stability calculations lead to the conclusion that the giant ELM occurs at the ballooning limit. Measurements of the edge pressure at the top of the H-mode pedestal,  $P_{ped}$ , on the other hand indicated that the ELM occurs when a critical  $P_{ped}/I_p$  value is reached. This is only compatible with the ballooning limit [3] if the width of the edge barrier  $\Delta_{bar} \propto I_p^{-1}$ , as predicted in the models where  $\Delta_{bar}$  is determined by the ion poloidal Larmor radius  $\rho_L$  [4], be that related to either the local thermal ions [5] or the fast ions [1,6].

In [1] the effects of isotopic mass and the applicability of several edge barrier models to the hot-ion H-mode plasmas were analysed using a large database containing both Deuterium-only (DD) and Deuterium-Tritium (DT) plasmas. It was shown that the edge data was best described by a model where  $\Delta_{bar}$  is determined by the fast ions with the largest poloidal Larmor radii. However, it was not possible to eliminate conclusively the thermal ion model. This database has now been enlarged to include discharges from a plasma shape scan [7], allowing to study the dependence of  $\Delta_{bar}$  on the edge shear. In addition the range of plasma currents was extended up to 6 MA.

In this paper the main results of [1] and [2] with respect to ELMs and edge pressure observations are summarised. The  $\Delta_{\text{bar}}$  scaling study is revised using the enlarged database.

## EDGE OBSERVATIONS

The large pressure gradients and large associated bootstrap currents that develop at the edge of a hot-ion H-mode plasma may lead both External Kinks and Ballooning modes unstable [2]. The OM is observed first, near the external kink marginal stability, then as the edge pressure increases and the ballooning limit is approached, the first giant ELM is observed (fig.1).

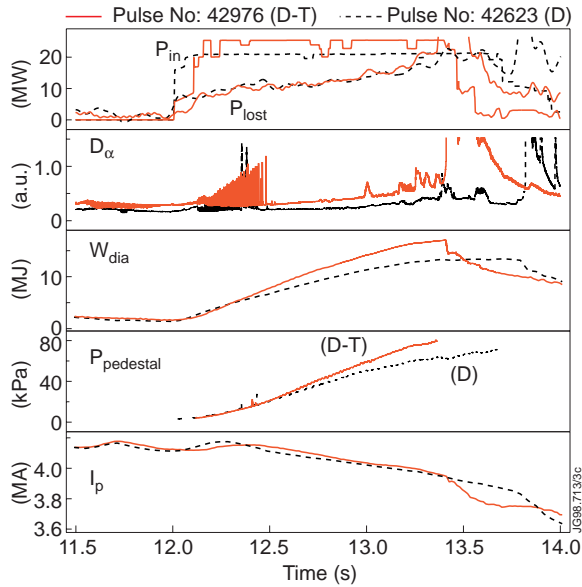


Fig.1: Record fusion DT discharge (with 50%T) compared to a DD reference discharge. The total plasma stored energy, neutron rate and the edge pedestal pressure (defined in this figure as  $P_{\text{ped}}(3.75\text{m})=n_e(T_e+T_i)$ ) rise until limited by a giant ELM.

Occasionally, smaller amplitude type I ELMs are also observed following large amplitude OM (figs.2-3). These earlier ELMs do not affect performance. These are not included in the  $\Delta_{\text{bar}}$  scaling studies. (A justification is given below.)

In DT, OMs occur earlier and the ELM-free period is typically shorter than in DD, however the differences are within the variability found for similar deuterium discharges. The most noticeable isotopic effect, discussed in detail in [1], is that the pedestal pressure rises more quickly in DT (fig.1).

## EDGE MEASUREMENTS

The direct measurement of the edge pressure gradient needed to determine the width of the edge transport barrier is not available at JET. In order to estimate  $\Delta_{\text{bar}}$ , the assumption is made that

The technique of current ramp-down described in [2] was found to be very effective to delay the OM. The flat-top  $I_p$  value is reduced with a rate  $dI_p/dt \sim 0.3-0.5$  during the heating phase. The lower  $j_{\text{edge}}$  increases stability to kink modes. This either delays the OM or decreases its amplitude (fig.2), with a substantial improvement in neutron yield.

In discharges, as in fig.1, where the OM has been delayed, the maximum core and edge pressures achieved depend solely on the timing of the 1<sup>st</sup> giant ELM (Provided the discharge is also sawtooth-free.). However, reducing the plasma current has the adverse effect of lowering the threshold for the onset of the giant ELM (fig.2). Modelling indicates that the earlier appearance of the giant ELM is consistent with the ballooning limit being reached earlier.

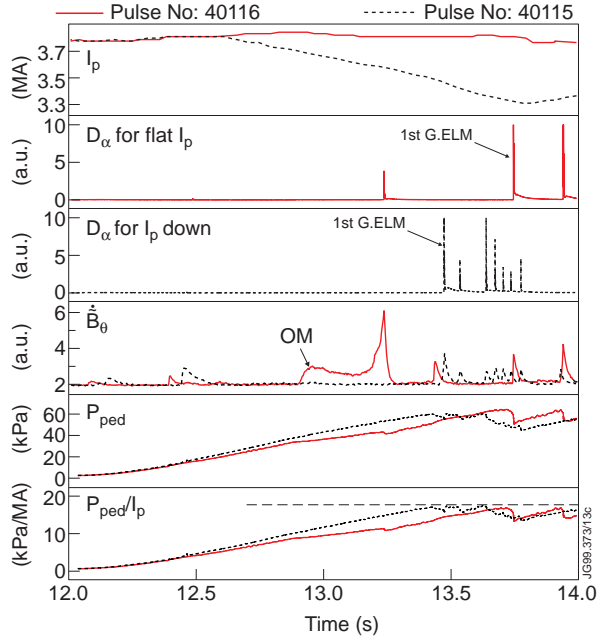


Fig.2: Comparison of discharges with  $I_p$  flat and  $I_p$  ramp-down. With  $I_p$  decreased the outer mode is delayed by 500 ms, allowing an improvement in the neutron rate of 45% [2]. However, the first giant ELM, which ends the high performance phase, occurs 300 ms earlier.

$\Delta_{\text{bar}} \approx P_{\text{ped}} / \nabla p$ , where  $P_{\text{ped}}$  is the pressure at the top of the edge pedestal. At the time of onset of the first giant ELM, it is assumed that  $\nabla p = \nabla p^{\text{crit}}$  is specified by the ballooning limit. For the majority of discharges, the outer most radius where all the measurements needed to calculate both electron and ion pressure are available is  $R=3.75\text{m}$ , inside the steep gradient region (fig.4). For the electron pressure,  $n_e$  is given by a line average determined from the edge channel of the interferometer, while  $T_e$  is a local measurement obtained from the electron cyclotron emission. The ion pressure is measured by the charge exchange diagnostics taking into account impurity dilution. The experimental uncertainty in  $P_{\text{ped}}$  is  $\pm 10\%$ .

The pressure at  $R=3.75\text{m}$  is only a suitable measurement of the pedestal height before an ELM, provided the ELM is not immediately preceded by a large amplitude long lived OM. The OM decreases the pressure of the bulk plasma,  $R \leq 3.75\text{m}$ . Thus the low pressure at  $R=3.75\text{m}$  observed at the onset of the early ELM that follows an OM (fig.2), appears to contradict the

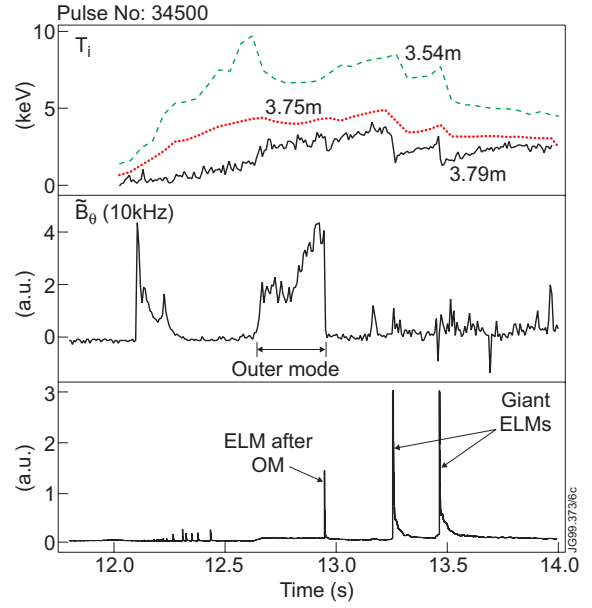


Fig.3: A hot-ion H-mode plasma limited by a large OM. The OM clamps  $T_i$  at  $R=3.75\text{m}$  where  $P_{\text{ped}}$  is normally measured. The OM triggers a small type I ELM.

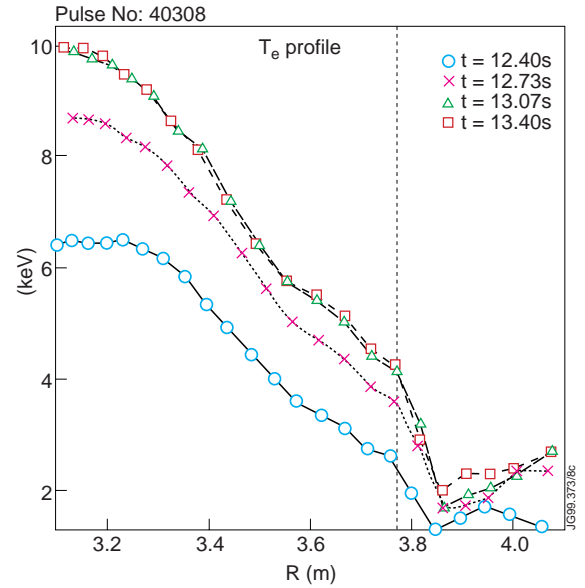


Fig.4: Electron temperature profiles measured during the ELM-free period in a DD discharge developed as reference for the high performance DTE1 campaign. The edge pedestal height and grad  $T_e$  increase in time.  $P_{\text{ped}}$  in this paper is calculated at  $R=3.75\text{m}$ .

hypothesis that the ELM occurs at the ballooning limit. In fact, in discharges where  $T_i$  measurements are available for  $R > 3.75\text{m}$ , the edge  $T_i$  increases during the OM (fig.3). This indicates  $\nabla p$  increases further out and may get to a value close to  $\nabla p^{\text{crit}}$ , at a radius where  $P_{\text{ped}}$  is not measured.

In the edge barrier scaling analysis discussed below, the  $P_{\text{ped}}$  includes dilution, i.e.  $P_{\text{ped}}(3.75\text{m}) = n_e T_e + n_d T_i$ . Only the maximum pressure attained just before the first giant ELM is considered.

## SCALING OF THE EDGE BARRIER

The linear dependence of the plasma pressure with  $I_p$  is most clearly obtained in the plasma current scans discussed in [2]. These experiments carried out at similar toroidal fields and triangularity show that the maximum plasma stored energy as well as the max  $P_{\text{ped}}$  attained at the time of the first giant ELM are linearly proportional to  $I_p$ , i.e.  $W_{\text{dia}} \propto I_p^\alpha$  and  $P_{\text{ped}} \propto I_p^\alpha$ , in both cases with  $\alpha \approx 1$ . In discharges where the OM has been delayed, the time of occurrence of the first giant ELM is also found to be proportional to the plasma current. For the same plasma configuration the maximum plasma stored energy increases with the level of input power, whilst the maximum value of  $P_{\text{ped}}$  is independent of power.

Similar conclusions can be made from the more general database discussed in [1] which includes both DD and DT pulses, in a large range of input powers and types of heating. The database now includes discharges from a plasma shape scan at constant  $I_p$  and  $s_{95}$  (the shear at the 95% flux surface) in the range 3 to 5 [7] and for completeness, the plasma current scan was extended to include plasmas with  $I_p > 4\text{MA}$ . These higher  $I_p$  plasmas are not available in the hot-ion H-mode regime. We have taken the 1<sup>st</sup> type I ELM observed in ELMy-H-mode discharges from a high plasma current experiment during the JET MKI divertor. (This is different from the analysis for ELMy H-modes discussed in [5] and [8] where  $P_{\text{ped}}$  is averaged over several subsequent ELMs.)

The whole database now contains the following plasma types. In DD: high performance discharges [7], plasma current scan [2], power step-down [9] and shape scan [7]. In DT: high performance with 50%T [10], alpha-heating experiments with 0-100%T [11] and discharges with DT injected into DD and DD injected into DT. Details of the auxiliary heating are given in [1], however within the experimental uncertainty the  $P_{\text{ped}}$  scaling given below are found to be independent of power level and the type of heating (either NBI only or a combination of NBI plus ICRH).

The scaling of  $P_{\text{ped}}$  with  $I_p$ , shear and  $\rho_L$  for both the thermal and fast ion models is shown in figures 5-8. The data show as a general trend that  $P_{\text{ped}} \propto I_p$  (fig.5), however  $P_{\text{ped}} \propto I_p * s_{95}$  gives a better representation of the shape scan discharges (fig.6). The straight lines in figs. 5-6 are linear fittings constrained through the origin for the following datasets: a) the  $I_p$  scan and b) the high performance DT discharges with 50%T.



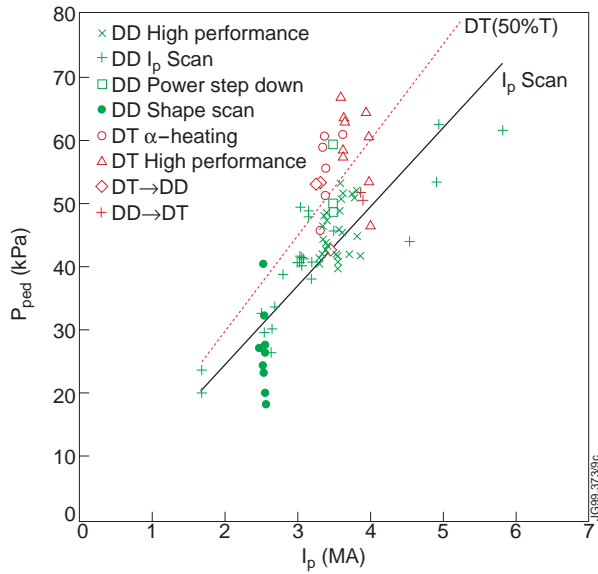


Fig.5:  $P_{ped}$  dependence on  $I_p$ . The linear fittings are for 3 sets of data:  $I_p$  scan, high performance DT discharges with 50%T.

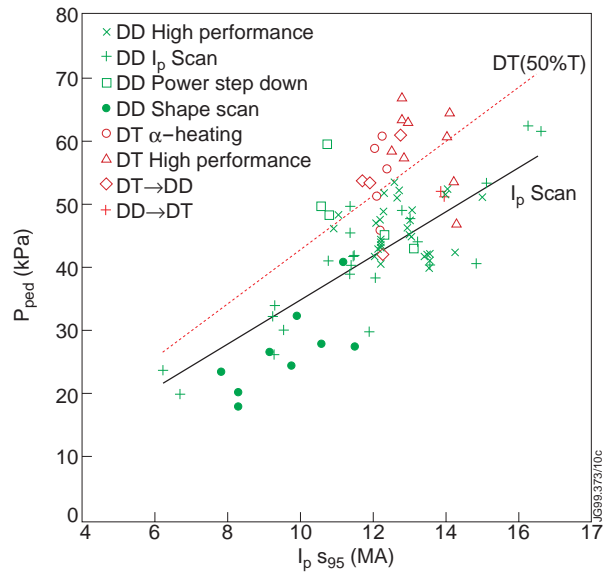


Fig.6:  $P_{ped}$  dependence on  $I_p$  and shear...

The larger  $P_{ped}$  observed for the DT- discharges suggest that fast particles may control  $\Delta_{bar}$ . Figs.7-8 show a comparison of the measured  $P_{ped}$  model predictions where  $\Delta_{bar} \propto \rho_L$ . If  $\Delta_{bar}$  is determined by thermal ions we expect  $P_{ped} \propto I_p^* s_{95}^* (\langle m_{th} \rangle * T_i)^{1/2}$  (fig.7). For the fast ion models the best fitting is obtained (as in [4]) for the components with the largest Larmor radius (Fig.8), where  $P_{ped} \propto I_p^* s_{95}^* (\text{Max}(m_{fast} * E_{fast}))^{1/2}$ .

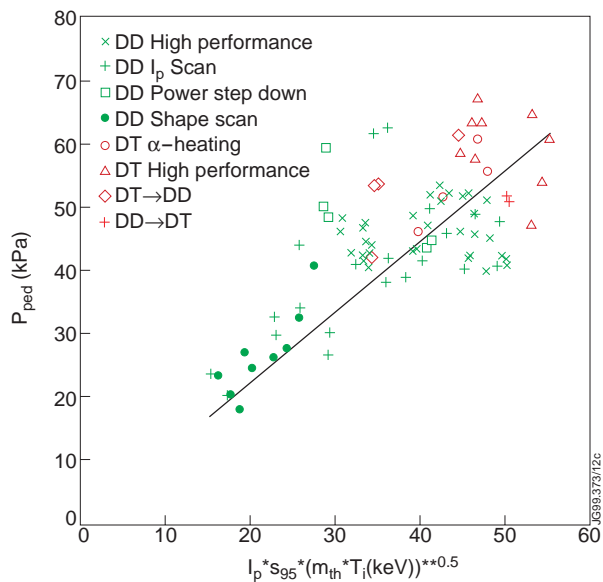


Fig.7:  $P_{ped}$  scaling in the thermal ion model

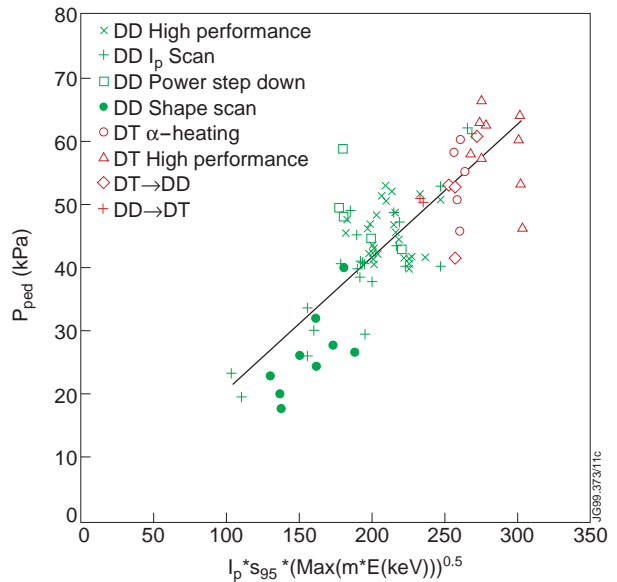


Fig8:  $P_{ped}$  scaling in the fast ion model weighted towards the components with largest Larmor radii.

The table shows the regression analysis with dependent variable  $P_{ped}$  and independent variable the thermal and fast models with and without shear. Slope is defined by  $P_{ped} = \text{slope} * \text{model}$ , the intercept is constrained to zero. The standard error is the corrected mean square residual and represents the scatter of individual measurements about the model. The adjusted  $R^2$  is the ratio of the sum of squares of the model to the sum of squares of residuals, adjusted for degrees of freedom for error. For a perfect fit  $R^2 = 1$ . Further explanation is given in [1].

Model	Obs	Slope	Standard Error	Adjusted $R^2$
$I_p(\text{MA}) * (m_{th} * T_i(\text{keV}))^{1/2}$	96	4.173	7.49	0.8784
$I_p(\text{MA}) * (\text{MAX}(m_{fast} * E_{fast}(\text{keV})))^{1/2}$	95	0.7455	6.25	0.9153
$I_p(\text{MA}) * S_{95} * (m_{th} * T_i(\text{keV}))^{1/2}$	96	1.140	8.87	0.8310
$I_p(\text{MA}) * S_{95} * (\text{MAX}(m_{fast} * E_{fast}(\text{keV})))^{1/2}$	95	0.2057	7.08	0.8940

Note that, whether or not  $s_{95}$  is included, the fast particle model gives a somewhat better fit than the thermal model, as indicated by lower standard error and higher  $R^2$ . However the difference is not large enough to allow us to exclude the thermal model.

## SUMMARY

In JET ELM-free discharges the edge pressure is clearly limited by edge MHD phenomena. In discharges where the OM is delayed the maximum core and edge pressures achieved depend on the time of onset of the 1<sup>st</sup> giant ELM.

At the time of onset of the first giant ELM, the following parameters were found to vary linearly with  $I_p$ :  $P_{ped}$  (measured at  $R=3.75\text{m}$ ),  $W_{dia}$  and the time of onset of the 1<sup>st</sup> giant ELM.  $P_{ped}$  varies linearly with shear (unlike the ELM regime where a quadratic dependence with shear has been reported [5,8]).

In the current ramp-down experiments the earlier onset of the first giant ELM indicates that the ELM occurs at the ballooning limit. However, an appropriated model for the edge pedestal is required where the width of the edge barrier depends on the plasma current.

The  $P_{ped}$  scaling with  $I_p$  is consistent with models where the edge  $\Delta_{bar}$  is determined by the poloidal ion Larmor radius. Both the thermal and fast ion models were assessed. The larger  $P_{ped}$  observed in DT discharges suggest that fast particles may control  $\Delta_{bar}$ . The best fitting is found for the fast ions weighted towards the ions with larger Larmor radius. However, the thermal ion model cannot be unambiguously excluded.

## REFERENCES:

- [1] Guo, H. Y et al, "Edge transport barrier in JET Hot-ion H-modes", 1999 to appear in Nucl. Fusion
- [2] Nave M.F.F. et al, Discharge optimisation and the control of edge stability, 1999 to appear in Nucl. Fusion
- [3] Pogutse O.P. and Yurchenko E. I. 1986 Rev. Plasma Phys. **11** 65
- [4] Shain K. C. and Crume E. C., 1989 Phys. Rev. Lett. **63** 2369
- [5] Saibene, G. et al, 1999 Nucl. Fusion **39** 1133
- [6] Parail V.V., Guo H.Y., Lingertat J., 1999 Nucl. Fusion **39** 369
- [7] The JET Team (presented by T.T.T. Jones) 1995 Plasma Phys. Control Fusion **37** A359
- [8] Bhatnagar, V. et al., 1999 Nucl. Fusion **39** (1999) 353
- [9] Marcus, F. B., 1997 Nucl. Fusion **37** 1067
- [10] Keilhacker, M. et al, 1998 Nuclear Fusion **39** 209
- [11] Thomas, P. R. et al, 1998 Phys. Rev. Lett. **80** 5548